Article

Cell Reports

Rapid Elevation in CMPF May Act As a Tipping Point in Diabetes Development

Graphical Abstract

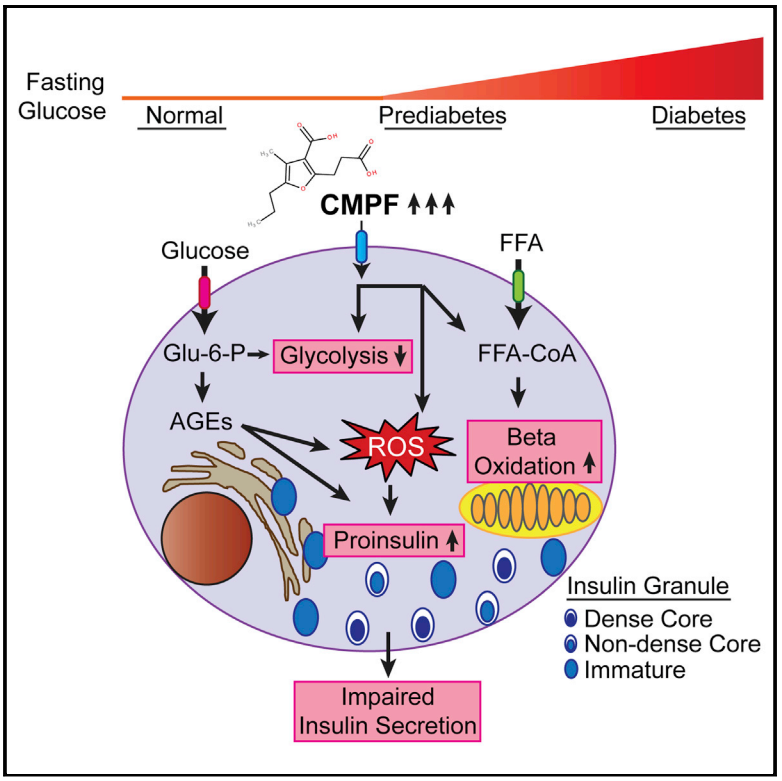

Highlights

- CMPF is significantly elevated in both prediabetes and type 2 diabetes
- Rapid elevation in circulating CMPF may accelerate diabetes development
- CMPF impairs glucose metabolism by introducing preferential fatty acid oxidation
- CMPF induces beta cell dysfunction shown as impaired insulin secretion

Authors

Ying Liu, Kacey J. Prentice, Judith A. Eversley, ..., Feihan F. Dai, Weiping Jia, Michael B. Wheeler

Correspondence

wpjia@sjtu.edu.cn (W.J.), michael.wheeler@utoronto.ca (M.B.W.)

In Brief

Liu et al. show that CMPF is significantly elevated in both prediabetes and type 2 diabetes. Rapid elevation in CMPF may represent the tipping point in beta cell function, playing a causal role in the conversion from prediabetes to type 2 diabetes.

Liu et al., 2016, Cell Reports *14*, 2889–2900
March 29, 2016
http://dx.doi.org/10.1016/j.celrep.2016.02.079

Cell Reports
Article

Rapid Elevation in CMPF May Act As a Tipping Point in Diabetes Development

Ying Liu,[1,4] Kacey J. Prentice,[1,4] Judith A. Eversley,[1] Cheng Hu,[3] Battsetseg Batchuluun,[1] Katherine Leavey,[2] Jakob B. Hansen,[1] David W. Wei,[1] Brian Cox,[2] Feihan F. Dai,[1] Weiping Jia,[3,*] and Michael B. Wheeler[1,*]
[1]Department of Physiology, University of Toronto, 1 King's College Circle, Medical Sciences Building, Room 3352, Toronto, ON M5S 1A8, Canada
[2]Department of Physiology, University of Toronto, 1 King's College Circle, Medical Sciences Building, Room 3360, Toronto, ON M5S 1A8, Canada
[3]Department of Endocrinology and Metabolism, Shanghai Jiao Tong University Affiliated Sixth People's Hospital, Shanghai 200233, China
[4]Co-first author
*Correspondence: wpjia@sjtu.edu.cn (W.J.), michael.wheeler@utoronto.ca (M.B.W.)
http://dx.doi.org/10.1016/j.celrep.2016.02.079

SUMMARY

Prediabetes, a state of mild glucose intolerance, can persist for years before a sudden decline in beta cell function and rapid deterioration to overt diabetes. The mechanism underlying this tipping point of beta cell dysfunction remains unknown. Here, the furan fatty acid metabolite CMPF was evaluated in a prospective cohort. Those who developed overt diabetes had a significant increase in CMPF over time, whereas prediabetics maintained chronically elevated levels, even up to 5 years before diagnosis. To evaluate the effect of increasing CMPF on diabetes progression, we used obese, insulin-resistant models of prediabetes. CMPF accelerated diabetes development by inducing metabolic remodeling, resulting in preferential utilization of fatty acids over glucose. This was associated with diminished glucose-stimulated insulin secretion, increased ROS formation, and accumulation of proinsulin, all characteristics of human diabetes. Thus, an increase in CMPF may represent the tipping point in diabetes development by accelerating beta cell dysfunction.

INTRODUCTION

Type 2 diabetes (T2D) is a progressive disease characterized by a significant decline in beta cell function, ultimately resulting in insufficient insulin secretion to meet metabolic demands (Weir and Bonner-Weir, 2004). In the early stages, increased demand due to insulin resistance induces a state of beta cell compensation mediated by increases in beta cell mass and insulin secretion to maintain euglycemia (Butler et al., 2003; Kahn, 2003; Weyer et al., 1999). Chronically high insulin demand, in combination with environmental and genetic factors, is thought to contribute to the initial stages of beta cell dysfunction, manifesting as impaired fasting glucose (IFG) and impaired glucose-tolerant (IGT) phenotypes, collectively termed prediabetes (Abdul-Ghani and DeFronzo, 2009; Kahn, 2003). These individuals have abnormalities in fasting blood glucose and/or a mild impairment during a glucose tolerance test (GTT; Bansal, 2015). Individuals with prediabetes are at a significantly elevated risk of developing T2D if their beta cell function continues to decline, with approximately 70% of prediabetic individuals eventually developing T2D (Pan et al., 1997).

Individuals with prediabetes can maintain a state of glucose intolerance for years before developing overt diabetes (Ferrannini et al., 2011; Tuomilehto et al., 2001). The deterioration to T2D occurs at vastly different rates for different individuals, though the conversion is directly correlated with a sudden and drastic impairment in glucose-stimulated insulin secretion (GSIS), independent of variables including BMI and insulin resistance (Ferrannini et al., 2004; Weir and Bonner-Weir, 2004). The mechanism underlying this tipping point of beta cell function, mediating the conversion from prediabetes to T2D, remains largely unknown. It has been suggested that chronic factors, including glucolipotoxicity, inflammation, endoplasmic reticulum (ER) stress, and/or oxidative stress may collectively exhaust the beta cell compensatory capacity, reducing beta cell mass and insulin secretion over time until compensation is no longer feasible (Abdul-Ghani et al., 2006; Jonas et al., 2009; Poitout and Robertson, 2008; Prentki and Nolan, 2006). However, this chronic picture does not account for acute instances of beta cell failure in response to insulin-resistant conditions. Gestational diabetes, a closely related condition to T2D that is also characterized by beta cell failure in response to insulin resistance, occurs acutely within weeks of insulin resistance onset and is rapidly resolved following parturition (Buchanan and Xiang, 2005). Therefore, we believe that underlying factors act to accelerate beta cell dysfunction in the conversion from prediabetes to overt diabetes.

Recently, 3-carboxy-4-methyl-5-propyl-2-furanpropanoic acid (CMPF) was found to be significantly elevated in the plasma of patients with gestational and T2D (Prentice et al., 2014). Further studies in animal models revealed a potential causal role of CMPF in diabetes development. However, the timing of the elevation in CMPF, and the role of CMPF in the deterioration of beta cell function during the progression to diabetes, before diabetes onset, has not yet been investigated. Here we performed a prospective study examining CMPF levels in human participants

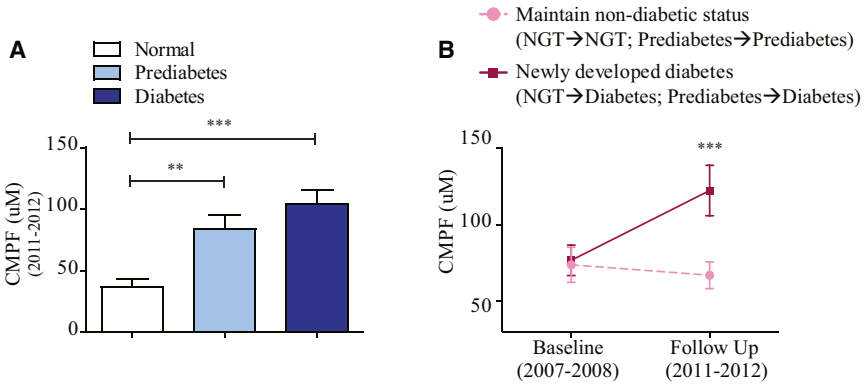

Figure 1. Plasma CMPF Is Elevated in Prediabetic and Diabetic Populations

(A) Plasma CMPF level was evaluated in human fasting plasma samples collected in 2011–2012; n = 50, 75, and 71 for normal, prediabetes, and diabetes groups, respectively.

(B) Change of plasma CMPF level was evaluated in plasma samples with both baseline (collected in 2007–2008) and follow-up (collected in 2011–2012). n = 65 for NGT → NGT and prediabetes → prediabetes, which represent maintenance of a non-diabetic state group; n = 57 for NGT → diabetes and prediabetes → diabetes, which represent a newly developed diabetes group.

Values are mean ± SEM, *p < 0.05, **p < 0.01, ***p < 0.001. See also Figure S1 and Tables S1–S4.

during a 5 year follow-up period and studies in prediabetic (high-fat diet, or HFD, and genetically predisposed) animal models to determine whether rapid elevation in plasma CMPF levels participates in the induction of beta cell failure and accelerates the pathological progression of diabetes.

RESULTS

Evaluation of Plasma CMPF in a Prospective Population

Plasma samples from the selected cohort (Figure S1A) of individuals at baseline (2007–2008; for clinical parameters, see Table S1) and follow-up (2011–2012; for clinical parameters, see Table S2) were evaluated for CMPF concentration. As anticipated, at the follow-up visit, the newly diagnosed diabetic population had significantly greater plasma CMPF concentration compared to normal glucose-tolerant (NGT) controls (103.9 ± 11.38 μM in diabetics versus 37.14 ± 6.350 μM in NGT controls, $p < 0.001$ ANOVA; Figure 1A). The levels of CMPF we detect in current diabetic patients are comparable to those in our previous report of Caucasians (Prentice et al., 2014). Prediabetic individuals also had a significantly greater CMPF compared to normal controls at this time point (84.14 ± 10.90 μM versus 37.14 ± 6.350 μM, $p < 0.01$ ANOVA; Figure 1A), suggesting that CMPF is associated with both diabetes and prediabetes (Figure S1B).

Analysis of CMPF in plasma samples from the same population at baseline, when all subjects were non-diabetic (Table S1), revealed a trend between plasma CMPF and future diabetes status. Individuals who were prediabetic or diabetic at the follow-up visit 4–5 years later tended to have increased levels of CMPF compared to controls at baseline, with levels being significantly elevated in future prediabetics ($p = 0.025$ future prediabetics versus future NGT, $p = 0.0718$ future diabetics versus future NGT, ANOVA; Table S3). We found that individuals with an increase in plasma CMPF concentrations between baseline and follow-up time points were at significantly higher risk of developing overt diabetes overall ($p = 0.00198$; Figure 1B; Table 1; Figure S1C). Those in the third and fourth quartiles of change, when adjusted for age, sex, BMI, and estimated glomerular filtration rate, had a significantly greater risk of developing diabetes compared to those in the lower quartiles (Table 1). Therefore, a large elevation in circulating CMPF concentration is associated with increased risk of diabetes development.

Elevated CMPF Impairs GSIS and Potentiates the Development of Diabetes in Rodent Models

To examine the role of rapid elevation in plasma CMPF in the context of pathological progression of diabetes, we used two models of diabetes development: HFD feeding to produce diet-induced obesity (DIO; Wang and Liao, 2012) and the genetic Ob/Ob mouse model (Lindström, 2010). Both models mimic the dyslipidemia and beta cell compensation for peripheral insulin resistance that is characteristic of diabetes development in the human population. These compensatory responses include increases in beta cell mass and insulin secretion, and they occur before the de-compensation and beta cell failure of overt diabetes (Lindström, 2010; Wang and Liao, 2012).

To establish our DIO diabetic model, we fed male CD1 mice a HFD composed of 60% kcal from fat or a sucrose-matched control chow diet for 6 weeks. To examine the role of CMPF, we then treated DIO mice with 6 mg/kg CMPF (Prentice et al., 2014) once daily for an additional 2 weeks while maintaining the mice on the HFD. DIO and chow mice injected with vehicle were used as controls (Figure S1D). Eight-week-old male Ob/Ob mice were used as a genetic model of diabetes development. These mice were injected with 6 mg/kg CMPF once daily for 2 weeks, as in the DIO model. Controls were treated with vehicle (Figure S1E). There was no difference in body weight or food consumption with CMPF treatment at the end of the treatment period in either model (data not shown).

After 2 weeks of CMPF treatment, DIO mice treated with CMPF (DIO-CMPF) exhibited even greater fasting blood glucose concentrations than DIO-control mice, with no significant difference in fasting plasma insulin levels (Figures 2A and 2B). Unlike the DIO model, CMPF had no additive effect on fasting hyperglycemia and hyperinsulinemia observed in the Ob/Ob-Control mice, perhaps due to the existing severity of hyperglycemia in Ob/Ob-controls (Figures 2C and 2D). In addition, DIO-CMPF mice had an even greater impairment in glucose tolerance than did DIO-controls, with a complete lack of GSIS during GTT (Figures 2E and 2G; Figure S2C). These results were mirrored in the Ob/Ob mice treated with CMPF (Ob/Ob-CMPF). Despite significant glucose intolerance in Ob/Ob-control mice, treatment with CMPF acted to further impair glucose tolerance (Figure 2F), which again correlated with a significant reduction in GSIS during the GTT (Figure 2H; Figure S2D). Together, these data

Table 1. Relation between the Change in CMPF Levels and the Risk of Future Diabetes Development

Change in CMPF Levels during 4–5 Year Follow-up Period	Development of Diabetes Compared to the Maintenance of a Non-diabetic State	
	Likelihood Ratio	p Value
First quartile	Baseline	–
Second quartile	1.74	0.188
Third quartile	5.41	0.02[a]
Fourth quartile	7.35	0.00669[a]
Continuous	9.57	0.00198[a]

Values were treated as both continuous and categorical (split by quartile of CMPF change, with the first quartile, the lowest observed change, employed as a baseline for comparison). Results are likelihood ratios for diabetes development, obtained from conditional logistic regression analysis. All models are adjusted for age, sex, BMI, and glomerular filtration rate. n = 65 for NGT → NGT and prediabetes → prediabetes (maintenance of a non-diabetic state). n = 57 for NGT → diabetes and prediabetes → diabetes (development of diabetes). All samples had both baseline and outcome measurements for CMPF.
[a]Value is statistically significant at $p < 0.05$.

suggest that CMPF acts to impair beta cell function to potentiate diabetes development.

To verify that the observed worsening in glucose tolerance is due to impaired beta cell function, we isolated islets from both models and performed GSIS assays ex vivo. Consistent with the observed impairment in GSIS during GTT, when we examined the glucose sensitivity of islets from individual mice, we found that islets from DIO-CMPF and Ob/Ob-CMPF mice had significantly reduced amplification in insulin secretion when stimulated with high glucose concentrations as compared to controls (Figures 2I and 2J; Figures S2A and S2B). The observed defect in GSIS was not associated with a reduction in total insulin content (Figures 2K and 2L) or differences in total insulin-positive area, as determined in whole pancreatic sections (Figures 2M and 2N), in either model, suggesting an alternate source of beta cell dysfunction, such as defective glucose utilization.

CMPF Treatment Impairs Glucose Metabolism by Metabolic Remodeling

The effect of CMPF on glucose metabolism was first assessed by measuring changes in mitochondrial membrane potential (MMP) in response to the acute addition of glucose. Islets from both chow and DIO-control mice exhibited a robust hyperpolarization of the MMP upon addition of 20 mM glucose (Figure 3A). Islets from DIO-CMPF mice, however, had a significantly blunted response (Figure 3A), corresponding to the observed impairment in GSIS. Remarkably, when the same assay was performed with the acute addition of 400 μM palmitic acid, the DIO-CMPF islets exhibited a greater hyperpolarization of the MMP than did either control (Figure 3B). This was also observed in islets from the Ob/Ob-CMPF mice compared to Ob/Ob-controls (Figures 3C and 3D). To further validate the changes in MMP in line with downstream substrate oxidation, we measured the oxygen consumption rate (OCR) in response to acute addition of glucose or palmitic acid by Seahorse-based metabolic flux analyses. Consistent with the observations in MMP, islets from DIO-CMPF mice exhibited significantly reduced glucose oxidation, and correspondingly significantly enhanced fatty acid oxidation, compared to DIO-controls (Figures 3E and 3F). To confirm that this effect of enhanced fatty acid utilization was not specific to murine islets, we treated human islets with vehicle, 400 μM palmitate, or 200 μM CMPF for 24 hr and evaluated their capacity for glucose oxidation. Pre-treatment with palmitate had no effect on glucose response compared to vehicle control; however, human islets pre-treated with CMPF had a significantly blunted response to the addition of glucose, consistent with the murine models (Figure 3G). In addition, when fatty acid oxidation was evaluated, we again observed a significantly enhanced response from CMPF pre-treated islets compared to both control and palmitic acid pre-treated islets (Figure 3H). In all assays, there was no effect on mitochondrial oxidative capacity with CMPF treatment, as indicated by identical elevations in the OCR after carbonyl cyanide 4-(trifluoromethoxy)phenylhydrazone (FCCP) stimulation between control and CMPF pre-treated human islets (Figures 3G and 3H), as well as no difference in expression of genes regulating mitochondrial oxidative capacity (see Figure 6C later). Overall, we have determined that CMPF induces a state of enhanced fatty acid utilization in islets, which reduces glucose metabolism, resulting in impaired GSIS.

CMPF Treatment Reduces Glycolysis and Increases Advanced Glycation End-Products and Oxidative Stress

The effect on fatty acid utilization prompted us to further examine glucose utilization in islets from CMPF-treated mice. We first evaluated the capacity for CMPF-treated islets to uptake glucose. CMPF treatment was associated with a significant increase in glucose uptake (Figure 4B), despite no changes in the expression of glucose transporter 2 (*Glut2*) at either the mRNA or the protein level (Figures S2E and S2F). In addition, we did not observe changes in expression of the rate-limiting enzyme in glycolysis, glucokinase (*Gck*), suggesting that CMPF likely does not alter the ability of cells to generate glucose-6-phosphate. CMPF treatment was associated with a significant reduction in glycolysis, as evaluated by the extracellular acidification rate (ECAR) in response to the addition of glucose using Seahorse (Figure 4A). Furthermore, the activity of pyruvate dehydrogenase (PDH) was also significantly reduced with CMPF treatment (Figure 4C). Thus, treatment with CMPF enhances glucose uptake but reduces glycolysis and impairs glucose utilization as an energy substrate in islets.

Previous studies have demonstrated that under hyperglycemic conditions, glucose can be shunted toward alternate pathways, including glycogen synthesis (Malaisse et al., 1993), the pentose phosphate pathway (PPP; Goehring et al., 2011; Spégel et al., 2013), and/or the hexosamine biosynthesis pathway (HBP; Kaneto et al., 2001; Shankar et al., 1998; Tang et al., 2000), which are all associated with beta cell dysfunction. The observed increase in glucose uptake, together with impaired metabolism, suggests that CMPF may induce shunting of glucose through these alternate pathways. To investigate this, we began by measuring transcript abundance of key rate-limiting enzymes regulating these processes. We did not observe differences in expression of glucose-6-phosphate dehydrogenase (*G6PD*; Zhang et al., 2010), gluconolactonase (*Rgn*), or glutamine fructose-6-phosphate amidotransferase (*Gfpt1*) (Figure S2E; Kaneto

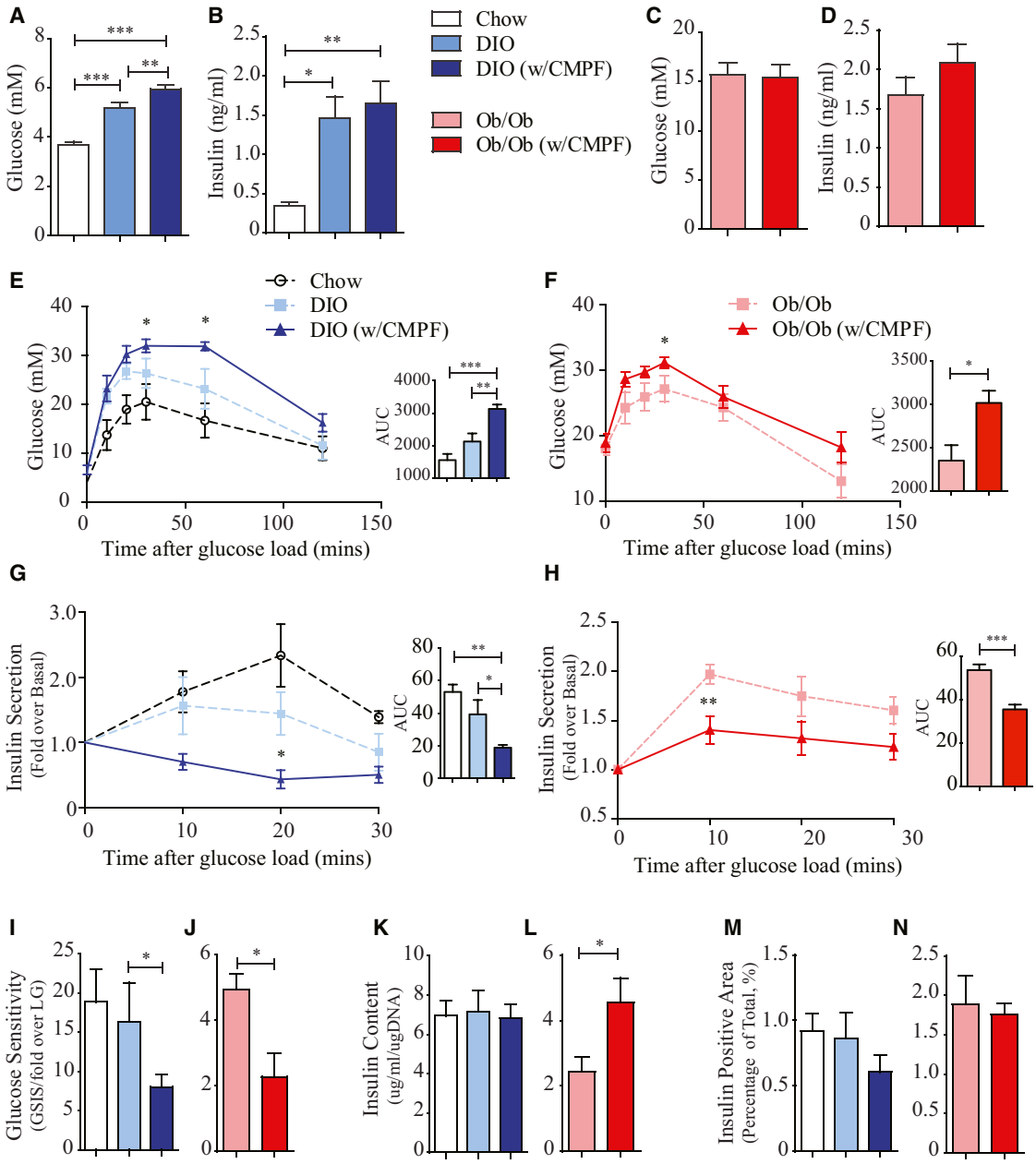

Figure 2. Elevated CMPF Impairs GSIS and Potentiates the Development of Diabetes in Rodent Models

(A–D) Fasting plasma glucose and insulin levels were checked in (A and B) DIO and (C and D) Ob/Ob mouse models, respectively.

(E–H) GTT was performed and corresponding insulin secretion was checked during i.p. GTT on (E and G) DIO and (F and H) Ob/Ob mouse models, respectively. Area under curve (AUC) inset for (E)–(H): n = 5–8 for GTT and n = 20–32 for others within each group.

(I–L) GSIS and total insulin content was examined in islets isolated from (I and K) DIO and (J and L) Ob/Ob mouse models, respectively.

(M and N) Quantitative analysis of insulin-positive area on pancreatic sections with insulin staining from (M) DIO and (N) Ob/Ob mouse models, respectively. n = 6–11.

Values are mean ± SEM, *p < 0.05, **p < 0.01, ***p < 0.001. See also Figure S2.

et al., 2001). To evaluate functionality of these pathways, we measured G6PDH activity, the rate-limiting enzyme for the PPP, and O-linked protein glycosylation, a read out of the HBP. There was no difference in G6PDH activity in CMPF-treated islets compared to controls (Figure 4D). We observed a reduction in total O-linked protein glycosylation in islets from Ob/Ob-CMPF mice compared to controls, suggesting decreased flux through the HBP (Figure 4E). Overall, these findings suggest that CMPF does not shunt excess glucose through regulated pathways. Consistent with this, we observed an increase in total

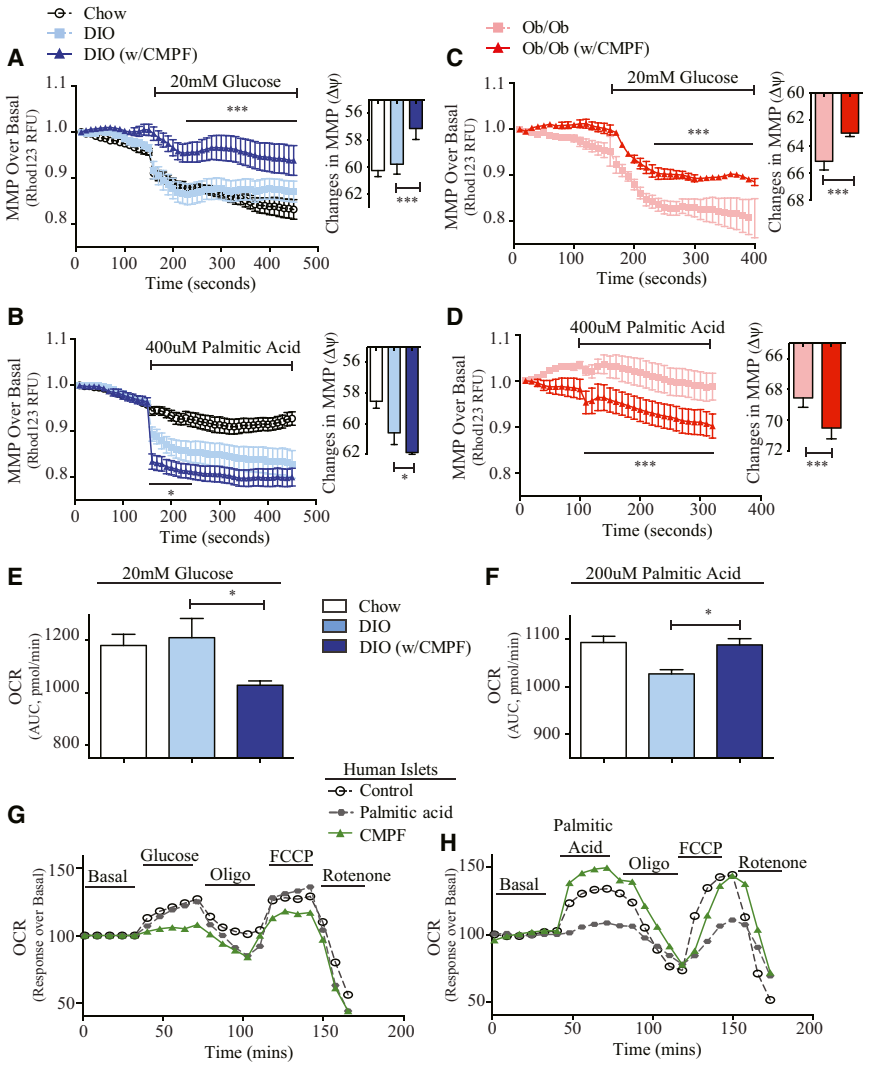

Figure 3. CMPF Treatment Impairs Glucose Metabolism by Metabolic Remodeling

(A and C) Glucose-induced hyperpolarization of the MMP was compared among islets isolated from the (A) DIO and (C) Ob/Ob mouse models.

(B and D) Palmitic acid-induced hyperpolarization of the MMP was compared among islets isolated from (B) DIO and (D) Ob/Ob mouse models. MMP changes ($\Delta\psi$) inset for (A)–(D).

(E and F) Seahorse-based metabolic flux analysis using the OCR as an output to evaluate energy substrate utilization on islets isolated from DIO mouse models upon loading of (E) 20 mM glucose and (F) 200 μM palmitic acid.

(G and H) Representative trace from a Seahorse experiment performed on human islets with additional loading of (G) 20 mM glucose and (H) 200 μM palmitic acid.

n = 4–12 for animal work and n = 3–4 for human islet work. Values are mean ± SEM, *$p < 0.05$, **$p < 0.01$, ***$p < 0.001$. RFU, relative fluorescence unit; AUC, area under curve.

glycoprotein content in the islets of CMPF-treated mice compared to controls (Figure 4F), likely due to aberrant protein glycation. Consistent with an increase in advanced glycation end-product (AGE) formation (Coughlan et al., 2011), as well as increased rates of fatty acid oxidation, islets isolated from both DIO-CMPF and Ob/Ob-CMPF mice exhibited significantly increased levels of reactive oxygen species (ROS) compared to controls (Figure 4G). This was not associated with the induction of islet apoptosis, as quantified by cleaved caspase-3/7 activity in islets ex vivo (Figure 4H). Thus, CMPF increases beta-oxidation and decreases glucose metabolism, increasing the formation of AGEs and ROS, to induce beta cell dysfunction.

CMPF Treatment Impairs Insulin Granule Maturation

Despite impaired beta cell glucose sensitivity and reduced GSIS in CMPF-treated mice, we observed no reduction in total insulin content compared to controls (Figures 2K–2N). To more closely examine the dynamics of insulin biosynthesis and storage with CMPF treatment, we used transmission electron microscopy (TEM). Islets from DIO-control mice exhibited characteristics of early beta cell dysfunction, including dilated ER (indicative of ER stress), hypertrophic mitochondria, and diminished insulin crystallization within granules (Figure 5A). This morphology was also observed in the islets of Ob/Ob-control mice (Figure 5B). Unexpectedly, the islets from CMPF-treated mice contained fewer typical insulin granules, characterized by a white halo surrounding a dense black core, than either control (Figures 5A and 5B). Observed granules included a large number of membrane-bound structures with homogenous content, not typical of mature secretory granules (called immature granules). The number of these structures was significantly increased with CMPF treatment relative to the number of typical insulin granules, particularly in the Ob/Ob model (Figures 5C and 5D). Given the size and orientation of the atypical granules, particularly their close relationship to the Golgi and plasma membrane, we predict that they may be misprocessed or immature insulin granules (Figure 5B, indicated by an asterisk). To determine whether this is the case, we performed immunogold electron microscopy (immunogold-EM) with antibody staining against insulin in islets from the Ob/Ob-control and Ob/Ob-CMPF mice. We found that all membrane-bound granule-like structures in islets from both mice contained insulin (Figure 5F). Given that the antibodies used for immunogold-EM and quantification of total insulin content are unable to distinguish between proinsulin and mature insulin, we finally quantified the amount of total proinsulin within the islets of CMPF-treated mice compared to controls. Consistent with the atypical granules being immature or containing misprocessed insulin, islets from CMPF-treated mice contained nearly twice as much proinsulin as did controls (Figure 5E).

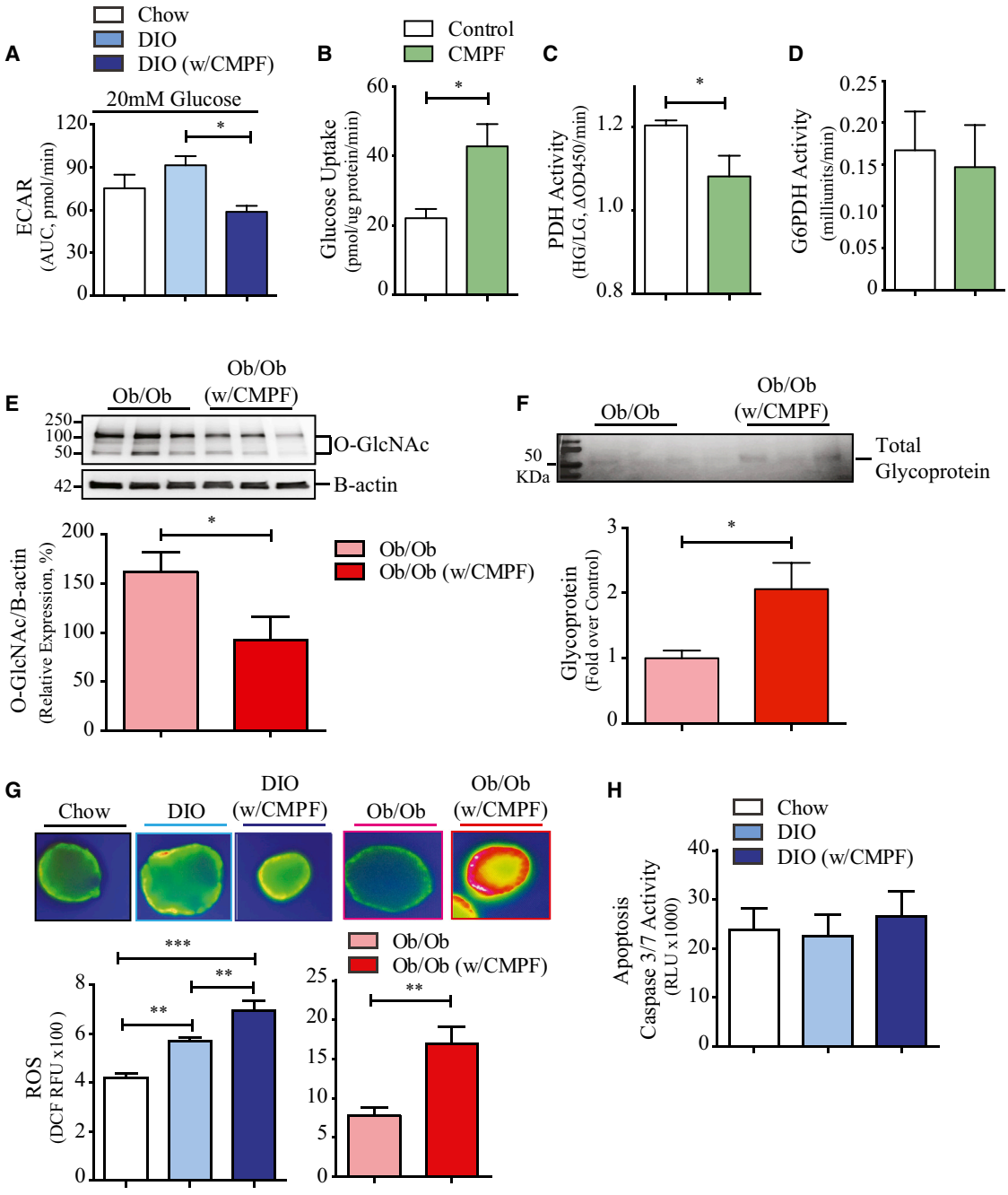

Figure 4. CMPF Treatment Reduces Glycolysis and Increases AGEs and Oxidative Stress

(A) Seahorse-based metabolic flux analysis using the ECAR as a readout to evaluate the glycolytic rate in islets isolated from DIO mouse models (n = 4–8).

(B–D) ^{14}C-2-deoxyglucose uptake (B) and enzymatic assays evaluating the activity of PDH (C) and G6PDH (D) performed on the primary mouse islet treated with or without 200 μM CMPF overnight. n = 3–4.

(E) Representative image and quantitative analysis of western blot analyzing O-linked glycosylation level in islets isolated from the Ob/Ob mouse model.

(F) Representative gel image and quantitative analysis of total glycosylated protein staining in islets isolated from the Ob/Ob mouse model.

(G) Representative images and quantitative analysis of ROS measurements taken with PTI fluorescence microscopy in islets isolated from DIO and Ob/Ob mouse models.

(H) Caspase-3/7 activity measured in islets isolated from the DIO mouse model. n = 4–15.

Values are mean ± SEM, *p < 0.05, **p < 0.01, ***p < 0.001. RFU, relative fluorescence unit; RLU, relative luminescence unit; O-GlcNAc, O-linked N-acetyl-glucosamine; LG, low glucose (2 mM); HG, high glucose (20 mM); AUC, area under curve. See also Figure S2.

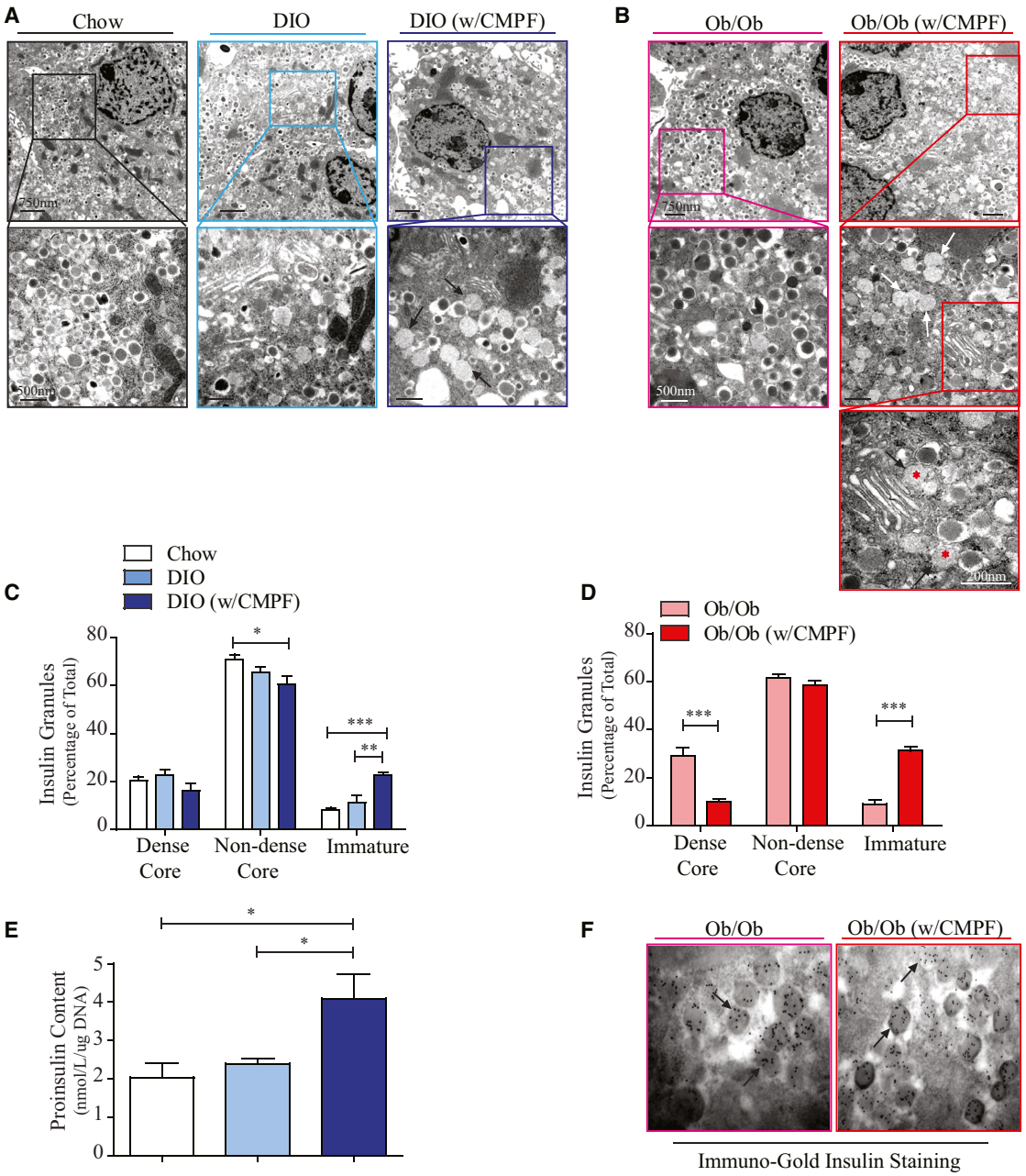

Figure 5. CMPF Treatment Impairs Insulin Granule Maturation

(A and B) Representative TEM images of islets isolated from (A) DIO and (B) Ob/Ob mouse models. Arrows and asterisks indicate the immature insulin granules.

(C and D) Quantitative analysis of the relative distribution of dense core versus immature insulin granules within beta cells from (C) DIO and (D) Ob/Ob mouse models.

(E) Proinsulin content measured in islets isolated from the DIO mouse model.

(F) Representative images of immunogold-EM insulin staining. Arrows indicate insulin-positive staining. n = 3 for TEM and n = 2 for immunogold-EM. n = 10–23 for proinsulin content.

Values are mean ± SEM, *p < 0.05, **p < 0.01, ***p < 0.001.

Thus, an increase in proinsulin due to impairment of granule maturation is likely responsible for the increased insulin content within islets.

Misprocessed or immature proinsulin-containing granules are characteristic of diabetes progression in humans based on numerous examinations of islets isolated from individuals with T2D postmortem (Masini et al., 2012; Sempoux et al., 2001). Furthermore, patients with T2D typically exhibit an increased proinsulin-to-insulin ratio, which has been suggested to be involved in impaired insulin signaling in diabetes (Grill et al.,

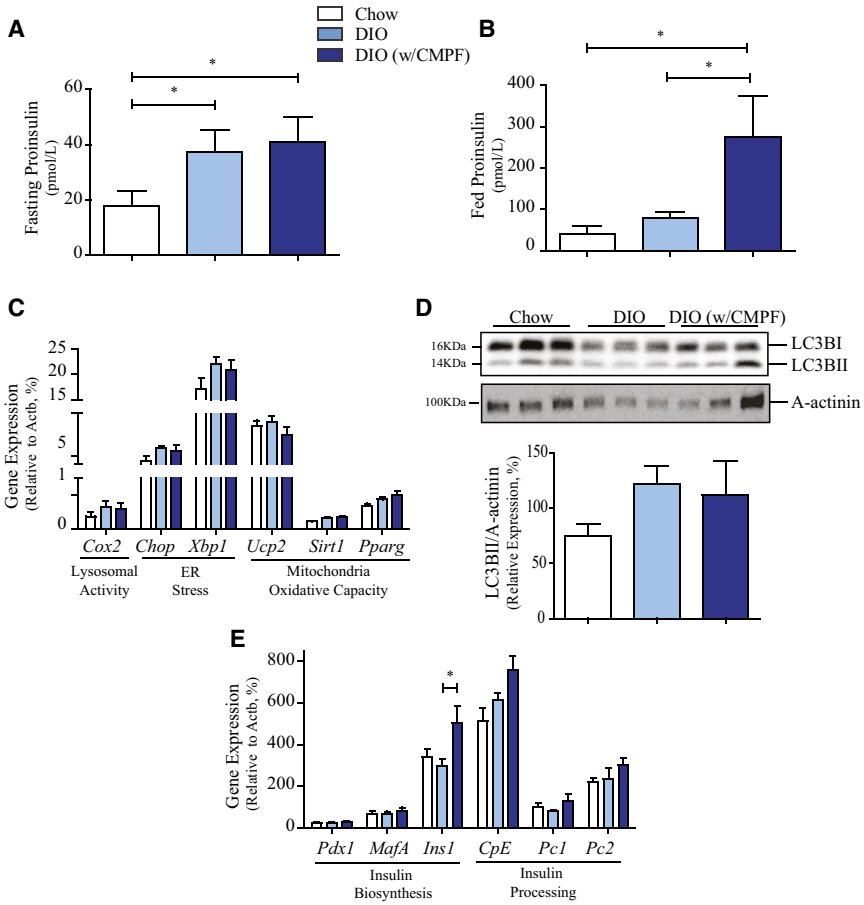

Figure 6. CMPF Treatment Increases Proinsulin

(A and B) Fasting (A) and fed (B) circulating levels of proinsulin were analyzed in the DIO mouse model. (C–E) qPCR analysis comparing gene expression levels of (C) genes involved in regulating oxidative and ER stress and mitochondrial oxidative capacity and (E) genes regulating insulin biosynthesis in islets isolated from the DIO mouse model. (D) Representative image and quantitative analysis of western blot, comparing the LC3BI and LC3BII protein expression levels in islets isolated from the DIO mouse model. n = 4–10.

Values are mean ± SEM, *p < 0.05. See also Figure S2.

from CMPF-treated mice with DIO or on an Ob/Ob background. Increased generation of immature insulin granules may therefore be attributed to increased levels of protein glycation, which is known to alter protein aggregation (Hull et al., 2004) and could therefore affect protein sorting and folding within granules.

DISCUSSION

The ultimate cause of T2D is a failure of the pancreatic beta cells to compensate for increased demands associated with insulin resistance. The pathological progression to diabetes is characterized by increases in beta cell mass, insulin biosynthesis, and insulin secretion in the compensatory period, followed by a decline in function and mass, ultimately resulting in overt diabetes (Weir and Bonner-Weir, 2004). This decline in beta cell function has been largely attributed to glucolipotoxicity, a combination of hyperglycemia and hyperlipidemia acting on the beta cell to increase ROS production and ER stress and ultimately to induce apoptosis (Poitout et al., 2010; Weir et al., 2009). However, glucolipotoxic conditions are not prevalent in the early stages of diabetes progression or even in the prediabetic period, when there are only mild changes in glucose tolerance and circulating free fatty acid levels (Bansal, 2015). In addition, in acute onset forms of T2D, such as gestational diabetes, a model of chronic deterioration in beta cell function does not match the clinical evolution of the disease.

In the present study, we examined the Shanghai Diabetes Study II (SHDS II) prospective cohort (Bao et al., 2010) for changes in plasma CMPF levels as patients were diagnosed with diabetes or prediabetes. We found that subjects who had rapid, large increases in plasma CMPF levels during the 4–5 year follow-up were at a significantly greater risk of developing overt diabetes in that short period. The levels of CMPF we detect in diabetics in the present population are comparable to our previous findings in gestational diabetes mellitus (GDM) and type 2 diabetic populations that were primarily Caucasian, suggesting this trend may not be specific to an Asian population (Prentice et al., 2014). Based on 2002). To examine the underlying cause of the increased number of immature granules, we began by investigating markers of impaired protein sorting in the granule maturation process. Despite significantly increased proinsulin in islets of CMPF-treated mice, circulating proinsulin was not significantly changed between DIO-CMPF mice and DIO-controls in the fasting state, suggesting the immature granules are not part of the constitutive pathway of secretion (Figure 6A). However, levels of circulating proinsulin were significantly increased in the fed state, indicating these immature granules are capable of secretion (Figure 6B). Together, these indicate that the defect may not lie in granule sorting or exocytosis. Immature granules may also accumulate due to differences in granule degradation (Uchizono et al., 2007). However, markers of lysosomal activity, the degradation machinery for misprocessed granules, including *Cox2* and LC3, were not significantly altered in islets from DIO-CMPF mice compared to controls (Figures 6C and 6D). Furthermore, there is no indication of elevated ER stress or activation of the unfolded protein response that would indicate aggregation of mis-folded insulin within the ER (*Chop* and *Xbp1* expression), a process that would also signal increased protein degradation (Figure 6C). Finally, we did not observe any differences in the transcript levels of the proteolytic genes responsible for insulin cleavage, including *Pc1/2* or *CpE* (Figure 6E). In conclusion, the insulin biosynthetic pathway appears to be intact in islets

our previous study into the effect of CMPF on impairing beta cell function (Prentice et al., 2014), we examined whether this dramatic increase in CMPF contributes to diabetes progression through promoting beta cell dysfunction in islets that are in a compensatory state. We used two models of diabetes development (DIO and Ob/Ob), and treatment with CMPF in both models produced a rapid decline in beta cell function, including worsened glucose tolerance, impaired GSIS both in vivo and in vitro, elevated ROS, and defective insulin processing in the absence of apoptosis, consistent with our previous observations in a lean model (Prentice et al., 2014). This decline in beta cell function was primarily associated with increased beta-oxidation and with impaired glucose metabolism, resulting in increased protein glycation, ROS, and insulin granule misprocessing or maturation, resulting in turn in aberrant proinsulin accumulation. Many of these effects may be due to the activation of a feedback compensatory mechanism, resulting in increased glucose uptake in response to reduced glycolysis and glucose metabolism after CMPF treatment. We attribute the differences in the islet phenotype between the lean and the obese models to obese islets having compensatory mechanisms in place to accommodate for CMPF's detrimental effect. Thus, CMPF has similar effects in both models, though the mechanism of action likely varies based on the phenotype of the islet when exposed to CMPF.

Normal pancreatic beta cell function is dependent on appropriate insulin cycling, including adequate insulin biosynthesis, appropriate insulin sorting, and crystallization, as well as insulin degradation to maintain a readily releasable pool (Uchizono et al., 2007). As newly formed secretory granules are formed from the trans-Golgi network, the budding structures contain various secretory proteins, including proinsulin and lysosomal proteins (Hou et al., 2009). As granules mature, sorting occurs and granules divide to remove non-proinsulin proteins into the lysosomes or the constitutive secretory pathway, leaving proinsulin to be cleaved into mature insulin and stored in releasable insulin pools. Previous work has demonstrated that this maturation process is perturbed in IGT and diabetes states in human patients, resulting in enhanced proinsulin accumulation and release (Grill et al., 2002; Sempoux et al., 2001). In the islets of DIO-CMPF and Ob/Ob-CMPF mice, we observe a profound accumulation of immature granules and an abundance of proinsulin content. These granules are capable of exocytosis, and mice exhibit a significant elevation in circulating proinsulin in the fed state compared to controls, similar to the human condition. We hypothesize that CMPF is altering the course of granule maturation in part through impairment of carbohydrate utilization. In the absence of glucose metabolism with CMPF treatment, glucose accumulates within the cell, resulting in abnormal formation of AGEs. In the beta cell, increased AGEs may be associated with aberrant insulin cross-linking, preventing appropriate folding and cleavage, to result in increased accumulation of immature insulin granules (Singh et al., 2001; Vitek et al., 1994). Future experiments are warranted to extend the understanding of the role AGEs play in the context of CMPF and islet function. Furthermore, induction of oxidative stress associated with AGE accumulation can act to impair insulin biosynthesis. ROS reduces Akt activation, resulting in diminished activity of key beta cell transcription factors PDX1 and MAFA and enhanced nuclear translocation of FOXO1, decreasing insulin transcription and processing (Kawamori et al., 2003). This is consistent with what was previously observed with CMPF treatment in chow-fed mice (Prentice et al., 2014). Altogether, altered insulin granule maturation in islets from CMPF-treated mice is likely caused by alterations to glucose utilization.

The progression from normal glucose tolerance to prediabetes occurs according to a fairly predictable series of events, including the induction of insulin resistance, enhanced insulin output under both basal and glucose-stimulated conditions, and gradual loss of first-phase insulin secretion, resulting in the prediabetic state. This prediabetic status with mild alterations in glucose tolerance can be maintained for years with only minimal impact on overall heath. The risk of transition from prediabetes to overt diabetes is about 10% annually, and when this occurs, the evolution is extremely rapid, with fasting blood glucose levels changing from 7–8 to 16–20 mmol/l within weeks (Weir and Bonner-Weir, 2004). This development is not associated with sudden changes in BMI or insulin resistance but is instead due to a tipping point in beta cell function with complete failure of compensation. Many argue that this tipping point is simply due to exhaustion of the beta cell following chronic exposure to glucolipotoxic conditions or ER or oxidative stress. However, this model is not consistent with acute forms of diabetes, such as gestational diabetes that occurs only weeks following induction of insulin resistance. Therefore, some independent factor may be the causal agent underlying this acceleration to beta cell failure. Our studies in a human population suggest that a rapid elevation in CMPF may cause this tipping point in beta cell dysfunction. The rapid elevation of CMPF in rodent models of diabetes progression accelerates diabetes development and produces a beta cell phenotype that closely resembles the human condition, including reduced glucose sensitivity (Mari et al., 2010), impaired insulin secretion (Cheng et al., 2013), elevation in proinsulin content and secretion (Grill et al., 2002; Sempoux et al., 2001), and ROS formation (Syed et al., 2011). Thus, elevated circulating CMPF may be a major risk factor for the development of beta cell failure and contribute to accelerate the progression of diabetes.

EXPERIMENTAL PROCEDURES

Study Population and CMPF Quantification

Fasting plasma samples were obtained from the SHDS II cohort of patients representing a cross-sectional population from six regions in Shanghai, China (Bao et al., 2010). Detailed information can be found in Supplemental Information.

Logistic Regression Analysis

Samples with missing a baseline, an outcome, or both values for CMPF were removed, and the data were log2 transformed. To assess the predictive power of the change in CMPF between the baseline and the outcome measurements on the progression to an overt diabetic state, the data were subjected to exact conditional logistic regression analysis using the *clogit* function (*survival* package from CRAN) in R 3.1.3. Patients who developed diabetes by the follow-up time point (starting from a NGT or prediabetic state) were compared to subjects who maintained their NGT or prediabetes diagnosis over the course of the study. Values were treated as both continuous and categorical (split by quartile of CMPF change) and were stratified by baseline age (binned: <35, 35–49, 50–64, or >65 years), sex (male or female), BMI (binned: <18.5, 18.5–25, 25–30, or 30–40 kg/m^2), and outcome glomerular filtration rate

(binned: <90 or >90 ml/min, as calculated by the modification of diet in renal disease formula). In addition, to assess the relationship between CMPF levels and additional clinical parameters, individual Spearman correlations were performed between these values in R 3.1.3. Variables found to be significantly associated with CMPF levels were further assessed, together in a linear model using the *glm* function.

Animal Models

All animals were housed in an environmentally controlled facility on a standard 12 hr light/dark cycle with free access to food and water. Seven-week-old male mice were purchased from Charles River Laboratories (CD1 mice) or Jackson Laboratory (Ob/Ob mice) and allowed to acclimate for 1 week before the study. CD1 mice were placed on a HFD with 60% kcal from fat (D12492, Research Diets) or a matched sucrose chow diet with 10% kcal from fat (D12450J, Research Diets) for 6 weeks. Mice were maintained on their respective diets while injected intraperitoneally once daily for 2 weeks with 6 mg/kg CMPF or vehicle (ethanol; Prentice et al., 2014). CMPF (Cayman Chemical) was prepared by dissolving in 70% ethanol to a stock concentration of 100 mM and diluted in sterile saline for injection. Ob/ob mice were maintained on a standard chow diet (Teklad diet 2018, Harlan Laboratories) throughout the 2 weeks of intraperitoneal (i.p.) injection with 6 mg/kg CMPF or vehicle. Mice were monitored for body weight weekly.

Glucose Tolerance Tests

At the end of the injection period, i.p. GTTs were performed on mice fasted for 14 hr overnight (Allister et al., 2013). The detailed procedure can be found in Supplemental Information.

Tissue and Islet Isolation, Insulin Secretion, Apoptosis, Total Glycoprotein, and Enzymatic Activity Measurements

Mice were anesthetized using isofluorane. Total blood volume was collected from the chest cavity following removal of the heart. Tissues were collected and flash frozen in liquid nitrogen for future analysis or fixed in a 4% formaldehyde solution for histology. The detailed procedure can be found in Supplemental Information. Cleaved caspase-3/7 assay was performed according to manufacturers' instructions using 30 islets (G8091, Promega). Total glycoprotein levels were measured by the Pierce Glycoprotein Staining Kit (catalog No. 24562, Thermo Fisher Scientific) in polyacrylamide gels according to manufacturers' instructions. Enzymatic activity assays (catalog No. MAK015, Sigma, and catalog No. ab109902, Abcam) were used to measure PDH and G6PDH activity, respectively, according to manufacturers' instructions.

Histology

Pancreata were fixed in 40% formaldehyde immediately following dissection. Tissue processing and immunostaining were performed as described previously (Luu et al., 2013). Images of each section were acquired using Aperio ImageScope at 20x magnification. Quantification of staining was calculated by using positive pixel count analysis (Aperio ImageScope).

Mitochondrial Membrane Potential

Islets isolated from mice were loaded with rhodamine 123 (25 μg/ml) in imaging buffer without glucose for 10 min. Islets were washed and placed in imaging chambers containing imaging buffer with no glucose. Images were taken at 10 s intervals at ex:511 nm by an Olympus IX70 inverted epi-fluorescence microscope in combination with an Ultrapix camera and a computer with Photon Technology International (PTI) imaging software, as previously described. Glucose was added to a final concentration of 20 mM to observe the correspondent change of MMP in cells. Alternately, palmitate conjugated to fatty acid-free BSA was added to a final concentration of 400 μM. Then, 5 mM NaN_3 was added to fully depolarize the MMP (Diao et al., 2008).

Reactive Oxygen Species

The level of H_2O_2 was determined using 2′,7′-dichlorodihydro-fluorescein diacetate (CM-H_2-DCFDA; Invitrogen), as previously described (Robson-Doucette et al., 2011). Briefly, isolated islets were loaded with DCFDA for 25 min in 2 mM glucose imaging buffer at 37°C. Islets were washed and imaged once at excitation (ex):475 nm for 20 ms.

Human Islets and Energy Substrate Utilization Measurements

Human islets from review board-approved healthy donors were provided by the IsletCore and the Clinical Islet Laboratory (University of Alberta). Islets were picked into low-glucose DMEM media (Gibco, Catalog No. 11885-084) with 10% fetal bovine serum, 1% penicillin/streptomyosin, and 1% L-glutamine and were treated with either control, 200 μM CMPF, or 400 μM palmitate for 24 hr (Prentice et al., 2014). Then, 70 islets were picked into each well of XF24 islet plates (Seahorse) and secured with a mesh cover, as previously described (Wikstrom et al., 2012). Cells were incubated in 2 mM glucose Kreb's Ring buffer (KRB) without bicarbonate for 1 hr before being loaded into the XF24 machine. OCR and ECAR were measured at 2 mM glucose, followed by either 20 mM glucose or 200 μM palmitate to measure substrate utilization and glycolytic rate, respectively. All islets were then treated with 5 μM oligomycin, 5 μM FCCP, 5 μM rotenone, and 5 μM antimycin A. Raw traces were normalized to basal respiration at 2 mM glucose. Glucose uptake was measured by 2-[^{14}C(U)]-deoxy-D-glucose (NEC720A, PerkinElmer); the detailed procedure can be found in Supplemental Information.

TEM and Immunogold-EM

Detailed procedures can be found in Supplemental Information.

Gene Expression

The detailed procedure can be found in Supplemental Information.

Western Blotting

The detailed procedure can be found in Supplemental Information.

Statistics

Statistical significance was assessed using either the Student's t test or one-way or two-way ANOVA for repeated measures, followed by a Bonferroni, Dunnett, and Tukey post-test comparison where required. $p < 0.05$ was considered significant. All data are mean ± SEM unless otherwise specified.

Study Approval

All animal experiments were approved by the Animal Care Committee at the University of Toronto, and animals were handled according to the Canadian Council of Animal Care guidelines. All human studies were approved by a Shanghai local ethics committee, and written informed consent was received from participants before inclusion in the study (Bao et al., 2010).

SUPPLEMENTAL INFORMATION

Supplemental Information includes Supplemental Experimental Procedures, two figures, and six tables and can be found with this article online at http://dx.doi.org/10.1016/j.celrep.2016.02.079.

AUTHOR CONTRIBUTIONS

Y.L., K.J.P., and M.B.W. designed the study. Y.L. and K.J.P. conducted experiments, acquired data, analyzed data, and wrote and edited the manuscript. J.A.E., B.B., J.B.H., and D.W.W. conducted experiments and reviewed the manuscript. C.H. and W.J. provided human plasma samples for analysis and reviewed the manuscript. K.L. and B.C. performed statistical analysis on data collected from human plasma samples and reviewed the manuscript. F.F.D. and M.B.W. reviewed the manuscript and contributed to the discussion.

ACKNOWLEDGMENTS

This study was funded by a CIHR operating grant (FDN-143219) to M.B.W. Y.L. and B.B. were supported by Banting and Best Diabetes Center postdoctoral fellowship awards. K.J.P. was supported by a CIHR doctoral research award. Some of the equipment used in this study was provided by the Diabetes Core Lab funded by the Canadian Foundation for Innovation and Ontario Research Fund, project number 30961. We thank Islet Core and Clinical Islet Laboratory (Alberta Islet Distribution Program, University of Alberta) for providing us with

human islets from review board-approved donors. The authors also thank Dr. Peter Arvan for his insightful advice regarding insulin granule maturation.

Received: September 4, 2015
Revised: December 15, 2015
Accepted: February 21, 2016
Published: March 17, 2016

REFERENCES

Abdul-Ghani, M.A., and DeFronzo, R.A. (2009). Pathophysiology of prediabetes. Curr. Diab. Rep. *9*, 193–199.

Abdul-Ghani, M.A., Tripathy, D., and DeFronzo, R.A. (2006). Contributions of beta-cell dysfunction and insulin resistance to the pathogenesis of impaired glucose tolerance and impaired fasting glucose. Diabetes Care *29*, 1130–1139.

Allister, E.M., Robson-Doucette, C.A., Prentice, K.J., Hardy, A.B., Sultan, S., Gaisano, H.Y., Kong, D., Gilon, P., Herrera, P.L., Lowell, B.B., and Wheeler, M.B. (2013). UCP2 regulates the glucagon response to fasting and starvation. Diabetes *62*, 1623–1633.

Bansal, N. (2015). Prediabetes diagnosis and treatment: a review. World J. Diabetes *6*, 296–303.

Bao, Y., Ma, X., Li, H., Zhou, M., Hu, C., Wu, H., Tang, J., Hou, X., Xiang, K., and Jia, W. (2010). Glycated haemoglobin A1c for diagnosing diabetes in Chinese population: cross sectional epidemiological survey. BMJ *340*, c2249.

Buchanan, T.A., and Xiang, A.H. (2005). Gestational diabetes mellitus. J. Clin. Invest. *115*, 485–491.

Butler, A.E., Janson, J., Bonner-Weir, S., Ritzel, R., Rizza, R.A., and Butler, P.C. (2003). Beta-cell deficit and increased beta-cell apoptosis in humans with type 2 diabetes. Diabetes *52*, 102–110.

Cheng, K., Andrikopoulos, S., and Gunton, J.E. (2013). First phase insulin secretion and type 2 diabetes. Curr. Mol. Med. *13*, 126–139.

Coughlan, M.T., Yap, F.Y., Tong, D.C., Andrikopoulos, S., Gasser, A., Thallas-Bonke, V., Webster, D.E., Miyazaki, J., Kay, T.W., Slattery, R.M., et al. (2011). Advanced glycation end products are direct modulators of β-cell function. Diabetes *60*, 2523–2532.

Diao, J., Allister, E.M., Koshkin, V., Lee, S.C., Bhattacharjee, A., Tang, C., Giacca, A., Chan, C.B., and Wheeler, M.B. (2008). UCP2 is highly expressed in pancreatic alpha-cells and influences secretion and survival. Proc. Natl. Acad. Sci. USA *105*, 12057–12062.

Ferrannini, E., Nannipieri, M., Williams, K., Gonzales, C., Haffner, S.M., and Stern, M.P. (2004). Mode of onset of type 2 diabetes from normal or impaired glucose tolerance. Diabetes *53*, 160–165.

Ferrannini, E., Gastaldelli, A., and Iozzo, P. (2011). Pathophysiology of prediabetes. Med. Clin. North Am. *95*, 327–339, vii–viii.

Goehring, I., Sauter, N.S., Catchpole, G., Assmann, A., Shu, L., Zien, K.S., Moehlig, M., Pfeiffer, A.F., Oberholzer, J., Willmitzer, L., et al. (2011). Identification of an intracellular metabolic signature impairing beta cell function in the rat beta cell line INS-1E and human islets. Diabetologia *54*, 2584–2594.

Grill, V., Dinesen, B., Carlsson, S., Efendic, S., Pedersen, O., and Ostenson, C.G. (2002). Hyperproinsulinemia and proinsulin-to-insulin ratios in Swedish middle-aged men: association with glycemia and insulin resistance but not with family history of diabetes. Am. J. Epidemiol. *155*, 834–841.

Hou, J.C., Min, L., and Pessin, J.E. (2009). Insulin granule biogenesis, trafficking and exocytosis. Vitam. Horm. *80*, 473–506.

Hull, R.L., Westermark, G.T., Westermark, P., and Kahn, S.E. (2004). Islet amyloid: a critical entity in the pathogenesis of type 2 diabetes. J. Clin. Endocrinol. Metab. *89*, 3629–3643.

Jonas, J.C., Bensellam, M., Duprez, J., Elouil, H., Guiot, Y., and Pascal, S.M. (2009). Glucose regulation of islet stress responses and beta-cell failure in type 2 diabetes. Diabetes Obes. Metab. *11* (*Suppl 4*), 65–81.

Kahn, S.E. (2003). The relative contributions of insulin resistance and beta-cell dysfunction to the pathophysiology of Type 2 diabetes. Diabetologia *46*, 3–19.

Kaneto, H., Xu, G., Song, K.H., Suzuma, K., Bonner-Weir, S., Sharma, A., and Weir, G.C. (2001). Activation of the hexosamine pathway leads to deterioration of pancreatic beta-cell function through the induction of oxidative stress. J. Biol. Chem. *276*, 31099–31104.

Kawamori, D., Kajimoto, Y., Kaneto, H., Umayahara, Y., Fujitani, Y., Miyatsuka, T., Watada, H., Leibiger, I.B., Yamasaki, Y., and Hori, M. (2003). Oxidative stress induces nucleo-cytoplasmic translocation of pancreatic transcription factor PDX-1 through activation of c-Jun NH(2)-terminal kinase. Diabetes *52*, 2896–2904.

Lindström, P. (2010). Beta-cell function in obese-hyperglycemic mice [ob/ob mice]. Adv. Exp. Med. Biol. *654*, 463–477.

Luu, L., Dai, F.F., Prentice, K.J., Huang, X., Hardy, A.B., Hansen, J.B., Liu, Y., Joseph, J.W., and Wheeler, M.B. (2013). The loss of Sirt1 in mouse pancreatic beta cells impairs insulin secretion by disrupting glucose sensing. Diabetologia *56*, 2010–2020.

Malaisse, W.J., Maggetto, C., Leclercq-Meyer, V., and Sener, A. (1993). Interference of glycogenolysis with glycolysis in pancreatic islets from glucose-infused rats. J. Clin. Invest. *91*, 432–436.

Mari, A., Tura, A., Natali, A., Laville, M., Laakso, M., Gabriel, R., Beck-Nielsen, H., and Ferrannini, E.; RISC Investigators (2010). Impaired beta cell glucose sensitivity rather than inadequate compensation for insulin resistance is the dominant defect in glucose intolerance. Diabetologia *53*, 749–756.

Masini, M., Marselli, L., Bugliani, M., Martino, L., Masiello, P., Marchetti, P., and De Tata, V. (2012). Ultrastructural morphometric analysis of insulin secretory granules in human type 2 diabetes. Acta Diabetol. *49* (*Suppl 1*), S247–S252.

Pan, X.R., Li, G.W., Hu, Y.H., Wang, J.X., Yang, W.Y., An, Z.X., Hu, Z.X., Lin, J., Xiao, J.Z., Cao, H.B., et al. (1997). Effects of diet and exercise in preventing NIDDM in people with impaired glucose tolerance. The Da Qing IGT and Diabetes Study. Diabetes Care *20*, 537–544.

Poitout, V., and Robertson, R.P. (2008). Glucolipotoxicity: fuel excess and beta-cell dysfunction. Endocr. Rev. *29*, 351–366.

Poitout, V., Amyot, J., Semache, M., Zarrouki, B., Hagman, D., and Fontés, G. (2010). Glucolipotoxicity of the pancreatic beta cell. Biochim. Biophys. Acta *1801*, 289–298.

Prentice, K.J., Luu, L., Allister, E.M., Liu, Y., Jun, L.S., Sloop, K.W., Hardy, A.B., Wei, L., Jia, W., Fantus, I.G., et al. (2014). The furan fatty acid metabolite CMPF is elevated in diabetes and induces β cell dysfunction. Cell Metab. *19*, 653–666.

Prentki, M., and Nolan, C.J. (2006). Islet beta cell failure in type 2 diabetes. J. Clin. Invest. *116*, 1802–1812.

Robson-Doucette, C.A., Sultan, S., Allister, E.M., Wikstrom, J.D., Koshkin, V., Bhattacharjee, A., Prentice, K.J., Sereda, S.B., Shirihai, O.S., and Wheeler, M.B. (2011). Beta-cell uncoupling protein 2 regulates reactive oxygen species production, which influences both insulin and glucagon secretion. Diabetes *60*, 2710–2719.

Sempoux, C., Guiot, Y., Dubois, D., Moulin, P., and Rahier, J. (2001). Human type 2 diabetes: morphological evidence for abnormal beta-cell function. Diabetes *50* (*Suppl 1*), S172–S177.

Shankar, R.R., Zhu, J.S., and Baron, A.D. (1998). Glucosamine infusion in rats mimics the beta-cell dysfunction of non-insulin-dependent diabetes mellitus. Metabolism *47*, 573–577.

Singh, R., Barden, A., Mori, T., and Beilin, L. (2001). Advanced glycation end-products: a review. Diabetologia *44*, 129–146.

Spégel, P., Sharoyko, V.V., Goehring, I., Danielsson, A.P., Malmgren, S., Nagorny, C.L., Andersson, L.E., Koeck, T., Sharp, G.W., Straub, S.G., et al. (2013). Time-resolved metabolomics analysis of β-cells implicates the pentose phosphate pathway in the control of insulin release. Biochem. J. *450*, 595–605.

Syed, I., Kyathanahalli, C.N., Jayaram, B., Govind, S., Rhodes, C.J., Kowluru, R.A., and Kowluru, A. (2011). Increased phagocyte-like NADPH oxidase and ROS generation in type 2 diabetic ZDF rat and human islets: role of Rac1-JNK1/2 signaling pathway in mitochondrial dysregulation in the diabetic islet. Diabetes *60*, 2843–2852.

Tang, J., Neidigh, J.L., Cooksey, R.C., and McClain, D.A. (2000). Transgenic mice with increased hexosamine flux specifically targeted to beta-cells exhibit hyperinsulinemia and peripheral insulin resistance. Diabetes *49*, 1492–1499.

Tuomilehto, J., Lindström, J., Eriksson, J.G., Valle, T.T., Hämäläinen, H., Ilanne-Parikka, P., Keinänen-Kiukaanniemi, S., Laakso, M., Louheranta, A., Rastas, M., et al.; Finnish Diabetes Prevention Study Group (2001). Prevention of type 2 diabetes mellitus by changes in lifestyle among subjects with impaired glucose tolerance. N. Engl. J. Med. *344*, 1343–1350.

Uchizono, Y., Alarcón, C., Wicksteed, B.L., Marsh, B.J., and Rhodes, C.J. (2007). The balance between proinsulin biosynthesis and insulin secretion: where can imbalance lead? Diabetes Obes. Metab. *9* (*Suppl 2*), 56–66.

Vitek, M.P., Bhattacharya, K., Glendening, J.M., Stopa, E., Vlassara, H., Bucala, R., Manogue, K., and Cerami, A. (1994). Advanced glycation end products contribute to amyloidosis in Alzheimer disease. Proc. Natl. Acad. Sci. USA *91*, 4766–4770.

Wang, C.Y., and Liao, J.K. (2012). A mouse model of diet-induced obesity and insulin resistance. Methods Mol. Biol. *821*, 421–433.

Weir, G.C., and Bonner-Weir, S. (2004). Five stages of evolving beta-cell dysfunction during progression to diabetes. Diabetes *53* (*Suppl 3*), S16–S21.

Weir, G.C., Marselli, L., Marchetti, P., Katsuta, H., Jung, M.H., and Bonner-Weir, S. (2009). Towards better understanding of the contributions of overwork and glucotoxicity to the beta-cell inadequacy of type 2 diabetes. Diabetes Obes. Metab. *11* (*Suppl 4*), 82–90.

Weyer, C., Bogardus, C., Mott, D.M., and Pratley, R.E. (1999). The natural history of insulin secretory dysfunction and insulin resistance in the pathogenesis of type 2 diabetes mellitus. J. Clin. Invest. *104*, 787–794.

Wikstrom, J.D., Sereda, S.B., Stiles, L., Elorza, A., Allister, E.M., Neilson, A., Ferrick, D.A., Wheeler, M.B., and Shirihai, O.S. (2012). A novel high-throughput assay for islet respiration reveals uncoupling of rodent and human islets. PLoS ONE *7*, e33023.

Zhang, Z., Liew, C.W., Handy, D.E., Zhang, Y., Leopold, J.A., Hu, J., Guo, L., Kulkarni, R.N., Loscalzo, J., and Stanton, R.C. (2010). High glucose inhibits glucose-6-phosphate dehydrogenase, leading to increased oxidative stress and beta-cell apoptosis. FASEB J. *24*, 1497–1505.